68M

00021759

CBGS
(3Hours)
Total Marks: 80

Q.1 a)

Sr. No:	Analog instrument	digital instrument
1	The instrument which gives output that varies continuously as quantity to be measured is known as analoginstrument.	The instrument which gives output that varies in discrete steps and only has finite number of values is known as digital instrument.
2	The accuracy of analog instrument is less.	The accuracy of digital instrument is more.
3	The analog instruments required more power.	The digital instruments required less power.
4	Sensitivity of analog instrument is more.	Sensitivity of digital instrument is less.
5	The analog instruments are cheap.	The digital instruments are expensive.
6	The resolution of analog instruments is less.	The resolution of digital instruments is more.

b)

1. **Operating Principle:** The transducer are many times selected on the basis of operating principle used by them. The operating principle used may be resistive, inductive, capacitive , optoelectronic, piezo electric etc.
2. **Sensitivity:** The transducer must be sensitive enough to produce detectable output.
3. **Operating Range:** The transducer should maintain the range requirement and have a good resolution over the entire range.
4. **Accuracy:** High accuracy is assured.
5. **Cost & availability:** The transducer should be cost effective, easy availability, reliable & should have low maintenanace.
6. **Errors:** The transducer should maintain the expected input-output relationship as described by the transfer function so as to avoid errors.

c) Which is fastest ADC and why?

d)

1. **Recurrent Sweep** - When the saw tooth, being an AC voltage, alternates rapidly, the display also occurs repetitively, giving out a lasting image. This operation is called recurrent sweep.
2. **Single Sweep** - The signal under study produces a trigger signal, which in turn produces a single sweep.
3. **Driven Sweep** - The saw tooth oscillator is a free running generator when operated independently. There is a chance that the sweep cycle may start after the signal cycle, thereby missing a part of the signal. Driven sweep removes this possibility because it is fixed by the signal itself. The sweep and signal cycles start at the same time.
4. **Triggered Sweep** - In a recurrent mode, the pattern is repeated again and again. In this mode the voltage rises to a maximum and then suddenly falls to a minimum. Electron beam moves slowly from left to right, retraces rapidly to the left and the pattern is repeated. The horizontal sweep action takes place whether the input signal is applied to the oscilloscope or not, and a horizontal line is displayed on the scope screen. A triggered sweep, on the other hand, does not start unless initiated by a trigger voltage, generally derived from an incoming signal.

$\alpha_p = 1$ we set $x_{pt1} = 0$ and $y_{pt1} = 0$ in Model 1). We solve this model (which is much easier). If the problem is feasible, the feasible solution is given as input to the Local Search Algorithm. Otherwise, we show that the problem is infeasible.

As a final remark, note that two alternative approaches for the Relax and Fix Algorithm used in other works could be as follows. After computing the fractional solution (x', y'), the initial solution $(\overline{x}, \overline{y})$ is determined by (i) applying rounding techniques or (ii) solving the integer problem restricted to the non-null variables of (x', y'). Our computational tests have shown that the proposed Relax and Fix Algorithm computes always significantly better cost solutions due to the obvious reason that is less restrictive (we fix to 1 some variables that are 1 in the LP solution and we keep in the model all other variables free) and, in many cases, the alternative approaches fail to provide a feasible solution.

VI. Computational Results

The problem instances used for these computational results assume that all client demand interfaces are of Ethernet 10 Gbps type and lightpaths can be either of type OTU-3 ($\delta_1 = 4$) or of type OTU-4 ($\delta_2 = 10$). Following a recent paper [22] (which proposes a cost model for different core network components, including optical components, together with predictions for technology evolution up to 2018), we have assumed a transparent reach of $l_1 = 2500$ km for lightpaths of type OTU-3 and of $l_2 = 2000$ km for lightpaths of type OTU-4. Note that the transparent reach of a lightpath is imposed by the optical degradation suffered not only on the fibers but also of the intermediate optical switching nodes. We consider that the optical degradation suffered by a lightpath while traversing an optical switching node is equivalent to the degradation incurred due to transmission over a 160 km of fiber link [23].

Concerning costs, since we do not consider regenerators in the middle of lightpaths, a lightpath cost is the sum of the muxponder costs of its end nodes. We assume a reference cost of 100 (*i.e.*, $c_{p1} = c_1 = 100$, for all $p \in P$) for a pair of muxponders required in a lightpath of type OTU-3 (muxponders grooming 4 Ethernet 10 Gbps demands into one OTU-3 lightpath). Then, we consider three possible cost values for the muxponder pairs required in the lightpaths of type OTU-4 (muxponders grooming 10 Ethernet 10 Gbps demands into one OTU-4 lightpath): a cost of 340 (representing an early introduction of this technology in the market with a very high price), a cost of 260 (representing a decrease of price due to increased market penetration) and a cost of 180 (representing a huge decrease of price due to advances in equipment manufacturing). Therefore, $c_{p2} = c_2 = 340$, 260 or 180, for all $p \in P$.

In all problem instances, we have considered the topology of the German Backbone Network (GBN), with 17 nodes and 26 edges (Fig. 4) and a fiber capacity of $|T| = 80$ wavelengths. The fiber lengths of GBN (also shown in Fig. 4) are such that it is always possible to set up a lightpath between any pair of nodes within the considered transparent reach values.

Concerning client demands, we have randomly generated 9 demand scenarios involving different numbers of demand pairs and different levels of aggregated demand. We have considered three values for the number of demand pairs $|D| \in \{50, 70, 90\}$ which represent around 37%, 51% and 66% of the total number of node pairs, respectively. For each value of $|D|$, three instances were randomly generated corresponding to three levels of aggregated demand. First, the end nodes of each demand pair d are randomly selected (considering all nodes with the same probability). Then, the aggregated demand value v_d of each pair d is an integer number randomly generated in the intervals $]0, 3000/|D|]$, $]0, 6000/|D|]$, $]0, 9000/|D|]$ and the corresponding instances are denoted by a, b, c, respectively. Note that, on average, the total number of Ethernet 10 Gbps client demands is 1500 on instances a, 3000 on instances b and 4500 on instances c. In general, the best solutions for instances of type a have few fully occupied fibers (*i.e.*, using the 80 wavelengths), while the best solutions for instances of type c have typically many fully occupied fibers.

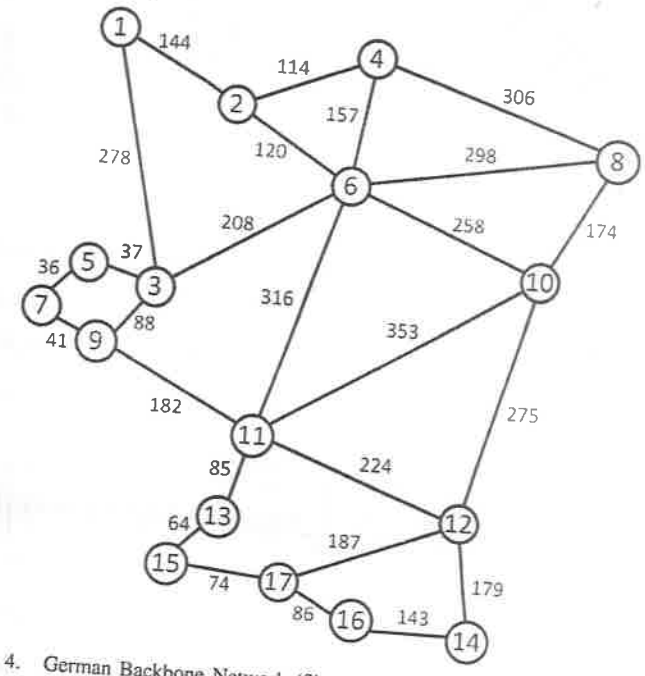

Fig. 4. German Backbone Network (fiber lengths in km).

All computations were performed using the optimization software Xpress-Optimizer Version 28.01.04 with Xpress Mosel Version 3.10.0, on a computer with processor Intel Core i7, 2.4 GHz and with 16 GB RAM.

Based on preliminary tests, Model 1 was shown to provide the best performance (either it reaches the same results in shorter runtimes or it reaches better results within the same runtime limit). Note that the MIR inequalities cannot be applied to Model 2 (one of the reasons why the proposed heuristic based on Model 1 is more efficient). So, we only present the results based on Model 1. Table I (for $c_2 = 180$), Table II (for $c_2 = 260$) and Table III (for $c_2 = 340$) present the lower bounds provided by the cost of the LP relaxation solutions of Model 1 without improvements (column M), Model 1 with increased demands (column $M + I$), Model 1 with increased demands and Knapsack inequalities (column $M + IK$), Model 1 with increased demands, Knapsack and MIR inequalities (column $M + IKM$), and Model 1 with

03

Q.2	a)	Explain working of LVDT and define its application in displacement measurement.

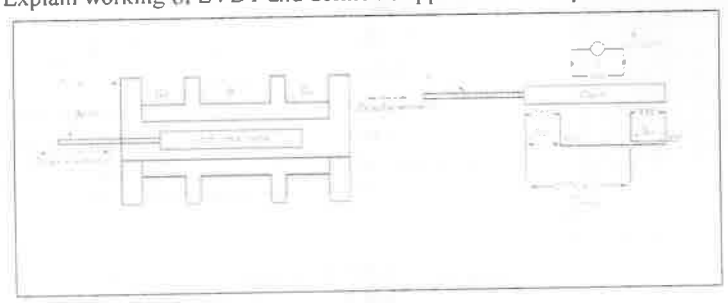

Principle of LVDT -

LVDT works under the principle of mutual induction and displacement, which is non-electrical energy being converted into electrical energy. It consists of a cylindrical former where it is surrounded by one primary winding in the center of the former and two secondary winding at the sides. The number of turns in both the secondary winding are equal, but they are opposite to each other, i.e., if the left secondary winding is in the clockwise direction, the right secondary windings will be in the anti-clockwise direction. Hence, the net output voltages will be the difference in voltages between the two secondary coils. The two secondary coils are represented as S1 and S2. A soft iron core is placed in the center of the cylindrical former which can move in to-and-fro motion as shown in the figure.

Working of LVDT –

As shown in the figure, an AC voltage with a frequency between (50-400) Hz is supplied to the primary winding. Thus, two voltages VS1 and VS2 are obtained at the two secondary windings S1 and S2 respectively. The output voltage will be the difference between the two voltages (VS1-VS2) as they are combined in series. Let us consider three different positions of the soft iron core inside the former.

Null Position – This is also called the central position as the soft iron core will remain in the exact center of the former. Thus the linking magnetic flux produced in the two secondary windings will be equal. The voltage induced because of them will also be equal. Thus the resulting voltage VS1-VS2 = 0.

Right of Null Position – In this position, the linking flux at the winding S2 has a value more than the linking flux at the winding S1. Thus, the resulting voltage VS1-VS2 will be in phase with VS2.

Left of Null Position – In this position, the linking flux at the winding S2 has a value less than the linking flux at the winding S1. Thus, the resulting voltage VS1-VS2 will be in phase with VS1.

From the working it is clear that the difference in voltages VS1-VS2 will depend on the right or left shift of the core from the null position. Also, the resulting voltage is in phase with the primary winding voltage for the change of the arm in one direction, and is 180 degrees out of phase for the change of the arm position in the other direction.

The magnitude and displacement can be easily calculated or plotted by calculating the magnitude and phase of the resulting voltage.

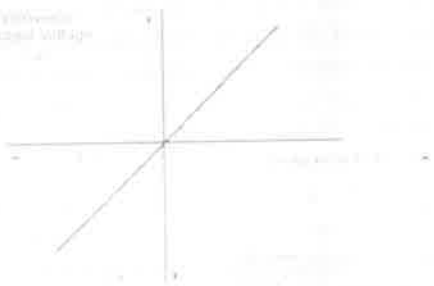

Q.2	b)	Dual Beam Oscilloscope Another method of studying two voltages simultaneously on the screen.

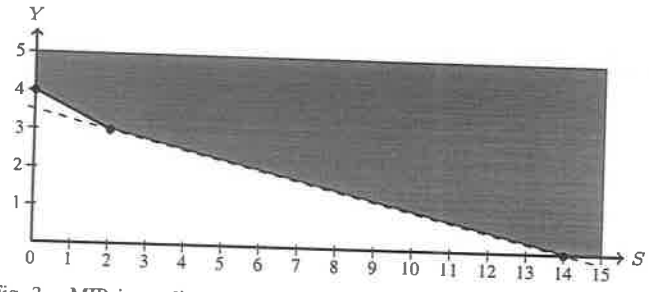

Fig. 3. MIR inequality for $X_M = \{(S, Y) \in \mathbb{R}_+ \times \mathbb{Z} \mid S + 4Y \geq 14\}$.

Algorithm 1 Relax and Fix Algorithm

1: Solve the LP relaxation of Model 1 with increased demand values
2: **repeat**
3: Identify and add violated inequalities
4: Solve the LP relaxation of the resulting model
5: **until** no new violated inequalities are found
6: Set (x', y') to the fractional solution
7: Set variables y_{pti} to one if $y'_{pti} = 1$ and run solver for at most $Time_1$ seconds
8: Set variables y_{pt2} to one if $y'_{pt2} = 1$ and run solver for at most $Time_1$ seconds
9: Set $(\overline{x}, \overline{y})$ to the best solution found

Example 6: Let $a = \delta_1 = 4$ and $v_d = 14$. In Fig. 3, the facet of the convex hull of X_{SMI} defined by the MIR inequality $S + 2Y \geq 8 \Leftrightarrow S \geq 2(4 - Y)$ is the line segment between points $(0, 4)$ and $(2, 3)$.

In order to identify the MIR inequalities, we have to decide whether each pair (p, t) belongs to $(\overline{P}, \overline{T})$ or not. We select one MIR inequality for each $i \in \{1, 2\}$ and each $d \in D$ in the following way: for a given relaxation solution, we compare the value of x_{pti} with $r \cdot y_{pti}$ and put (p, t) in $(\overline{P}, \overline{T})$ if $x_{pti} > r \cdot y_{pti}$.

V. Hybrid Heuristic Procedure

As we are dealing with an NP-hard problem, one can hardly expect to solve all problem instances to optimality within reasonable runtime limits. Hence, in this section, we propose a heuristic procedure combining two algorithms: a Relax and Fix Algorithm that aims at finding an initial feasible solution and a Local Search Algorithm that aims at improving the feasible solution provided by the first algorithm.

In the Relax and Fix Algorithm (see Algorithm 1), we start by determining a fractional solution (x', y') (steps 1 to 6) in the following way: we solve the LP relaxation of Model 1 with the demand values increasing rule as defined in the previous section (Step 1) and, then, we add the valid inequalities that are violated and solve again the LP relaxation until no new violated inequalities are found (steps 2 to 5). The addition of the valid inequalities follows the order: Knapsack, MIR, and Clique inequalities (the computational tests have shown that this order leads to the smallest number of added inequalities, keeping the size of the models as small as possible).

Then, some of the y binary variables with value 1 in the fractional solution (x', y') are fixed to 1 and the resulting restricted integer model is solved with a runtime limit of $Time_1$. We have considered two fixing strategies: (i) fix to 1 all y_{pti} variables *i.e.*, for both types of lightpaths $i \in \{1, 2\}$ that have value 1 (step 7) and (ii) fix to 1 the y_{pt2} variables (*i.e.*, only for lightpaths of type 2) that have value 1 (step 8). In the first case, we have a more restrictive integer model that is solved in shorter runtime but has a lower probability of being feasible. In the second case, we have a less restrictive integer model that is solved in longer runtime but has a higher probability of being feasible. If both approaches provide a feasible solution, the best one is chosen (step 9).

Algorithm 2 Local Search Algorithm

1: **repeat**
2: Fix the variables y_{pt1} to one if $y'_{pt1} = 1$ and $\overline{y}_{pt1} = 1$
3: Add inequality (V.1)
4: Run solver for at most $Time_2$ seconds
5: If a better solution is found then update $(\overline{x}, \overline{y})$
6: **until** No improvement is obtained

The Local Search Algorithm (see Algorithm 2) takes as input the best solution, denoted by $(\overline{x}, \overline{y})$, obtained by the previous algorithm, and searches for better solutions in a neighborhood of this solution. This neighborhood is characterized by those solutions such that the number of lightpaths assigned to a path and/or to a wavelength that differs from the one in $\overline{y}$ is at most Δ. From a modeling point of view, this corresponds to adding (in step 3) a constraint ensuring that at most Δ variables y_{pti} can have a different value from the value they have in solution $(\overline{x}, \overline{y})$, which is given by $\overline{y}_{pti}$:

$$\sum_{p \in P, t \in T, i \in \{0,1\} | \overline{y}_{pti} = 0} y_{pti} + \sum_{p \in P, t \in T, i \in \{0,1\} | \overline{y}_{pti} = 1} (1 - y_{pti}) \leq \Delta. \quad \text{(V.1)}$$

The first term counts the number of variables y_{pti} that have a value 0 in $(\overline{x}, \overline{y})$ and flip their value to 1 while the second term counts the number of variables y_{pti} that have a value 1 in $(\overline{x}, \overline{y})$ and flip their value to 0. Then, we solve the resulting model for at most $Time_2$ seconds (step 4), update the best feasible solution if a better solution is found (step 5) and repeat the process until no improvement is obtained (step 6). In order to speed up the algorithm, we fix to 1 all variables that have value 1 in both the fractional and the best solution (step 2).

Note that Δ, $Time_1$ and $Time_2$ are parameters of the heuristic procedure. For the problem instances considered in the computational results, and after some preliminary computational tests, we have observed that the best trade-off between the quality of the final solution and the runtime to find it, on average, was obtained with the parameters $\Delta = 5$, $Time_1 = 1500$ seconds and $Time_2 = 600$ seconds.

An important issue is whether the Relax and Fix Algorithm is able to find a feasible solution when the problem is feasible. We added a last step to the Relax and Fix Algorithm that is run when none of the fixing strategies finds a feasible solution. In this step, paths that are common to both lightpath types are only considered for type 2 (*i.e.*, for $p \in P$ such that

		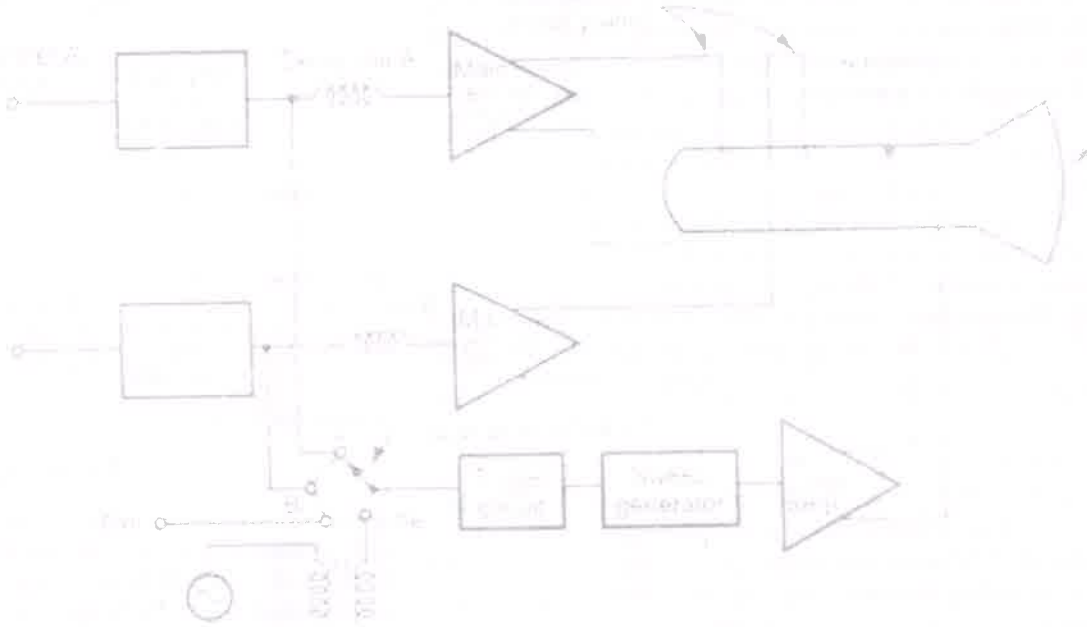 The oscilloscope has two vertical deflection plates and two separate channels A and B for the two separate input signals. Each channel consists of a preamplifier and an attenuator. A delay line. main vertical amplifier and a set of vertical deflection plates together forms a single channel. There is a single set of horizontal plates and single time base circuit. The sweep generator drives the horizontal amplifier which in turn drives the plates. The' horizontal plates sweep both the beams across the screen at the same rate. The sweep generator can be triggered internally by the channel A signal or .channel B signal. Similarly it' can also be triggered from an external signal or line frequency signal. This is possible with the help of trigger selector switch, a front panel control. Such an oscilloscope may have separate time base circuit for separate channel. This allows different sweep rates for the two channels but increases the size and weight of the oscilloscope.
Q.3	a)	Draw and explain Hay bridge and its application for measurement of inductances.

These inequalities can be added a priori to the models or added dynamically, that is, an inequality is added when the fractional solution violates that inequality. These inequalities can also be extended to the case where more than two types of lightpaths are considered, as described in [20].

2) Clique Inequalities: A common relaxation, when incompatibility between binary variables is considered (*i.e.*, variables that cannot simultaneously assume value 1 in the solution) is the vertex packing set. These incompatibilities are often called conflicts and are represented in a conflict graph where nodes represent variables and edges represent incompatibility between two binary variables. Given a conflict graph $G = (\mathcal{N}, \mathcal{E})$, the vertex packing set [21] is defined as $X_{VP} = \left\{ z \in \{0,1\}^n \mid z_u + z_v \leq 1, (u,v) \in \mathcal{E} \right\}$, where z_u is a binary variable indicating whether node u is selected or not and $n = |\mathcal{N}|$.

Here, each node u of the conflict graph in $\mathcal{N}$ is a triple (p,t,i) that corresponds to a variable y_{pti} and there is an edge in $\mathcal{E}$ between two nodes (p,t,i) and (p',t',i'), if the corresponding variables cannot be set simultaneously to one, that is, $y_{pti} + y_{p't'i'} \leq 1$. Constraints (III.5) impose incompatibility between all pairs of variables representing lightpaths that use the same wavelength on the same fiber. A complete description of the convex hull of X_{VP} is not known and since optimizing a linear function over X_{VP} is NP-hard, there is no much hope in finding such a description. Nevertheless, families of valid inequalities are known [18] and one of the most well-known families is the set of clique inequalities. A clique in a graph is a subset of nodes such that for each pair of nodes in the subset there exists an edge connecting them. In the present case, a clique is a set of variables that are pairwise incompatible. Then, the following result stands:

Proposition 4: If $C \subset \mathcal{N}$ is a clique in the conflict graph G, then the inequality (called clique inequality)

$$\sum_{(pti) \in C} y_{pti} \leq 1, \tag{IV.2}$$

is valid for X.

A maximal clique is a clique that cannot be extended by including one more adjacent node, meaning it is not a subset of a larger clique. It is well-known that only clique inequalities associated with maximal cliques need to be considered [21]. As the number of clique inequalities can increase exponentially with the number of variables, this family of inequalities is, in general, added dynamically.

Our preliminary experiences showed that there are too many clique inequalities resulting in too large models (some of these clique inequalities can also be identified and added automatically by the solver). Therefore, we focused on deriving clique inequalities that use the knowledge of the structure of the GRWA network design problem. A family of clique inequalities that was shown to be effective in cutting off fractional solutions with a small number of inequalities is as follows. We define a Y-structure of a network as a subgraph which contains four nodes with the structure shown in Fig. 2 where node B is the central node. Considering the conflicts

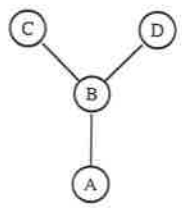

Fig. 2. Y-structure subgraph.

arising from Y-structures, for $t \in T$, the clique incquality

$$\sum_{p \in P_B} \sum_{i=1}^{2} y_{pti} \leq 1,$$

is valid for X where

$$P_B = \left\{ p \in P \mid p \text{ passes through central node } B \right\}.$$

In order to identify these clique inequalities, we identify each Y-structure on the fiber network defined by the graph $G = (N, E)$ (note that each node on N with a degree of 3 is the central node of a Y-structure) and add the value of all y_{pti} variables representing paths that include two edges of the Y-structure. If the total value is greater than one, then the corresponding clique inequality (IV.2) is added.

3) Mixed Integer Rounding (MIR) Inequalities: MIR is a technique to derive strong valid inequalities for mixed integer sets. The well-known MIR inequalities [18] can be stated as follows.

Proposition 5: Consider the simple mixed integer set $X_{SMI} = \{(S,Y) \in \mathbb{R}_+ \times \mathbb{Z} \mid S + aY \geq b\}$ where $a, b \in \mathbb{R}_+$ are arbitrary constants. The inequality (called MIR inequality)

$$S \geq r\big(\lceil b/a \rceil - Y\big), \tag{IV.3}$$

is valid for X_{SMI}, where $r = b - (\lceil b/a \rceil - 1)a$.

Next, we apply this proposition to derive valid inequalities for X. In order to do that, we define mixed integer sets of the form of X_{SMI} that result from the relaxation of X. For each lightpath type $i \in \{1,2\}$, each demand pair $d \in D$ and considering a subset of paths $\overline{P} \subset P_d$ and a subset of wavelengths $\overline{T} \subset T$, we use constraints (III.2), (III.3) and (III.4) to show that:

$$\sum_{p \in P_d} \sum_{t \in T} \sum_{j \in \{1,2\} | j \neq i} \alpha_{pj} x_{ptj} + \sum_{p \in P_d \setminus \overline{P}} \sum_{t \in T \setminus \overline{T}} \alpha_{pi} x_{pti}$$

$$+ \sum_{p \in \overline{P}} \sum_{t \in \overline{T}} \alpha_{pi} \delta_i y_{pti} \geq \sum_{p \in P_d} \sum_{t \in T} \sum_{j=1}^{2} \alpha_{pj} x_{ptj} = v_d.$$

where $\alpha_{p1} = 1$ and $\alpha_{p2} = \alpha_p$. To obtain this inequality, we start from constraint (III.2) and replace variables x_{pti} (with $p \in \overline{P}$ and $t \in \overline{T}$) with the term $\delta_i y_{pti}$ (if $i = 1$) coming from constraints (III.3) or the term $\alpha_p \delta_i y_{pti}$ (if $i = 2$) coming from constraints (III.4). In this way, for a given type i and demand pair d, the inequality (IV.3) holds by setting

$$S = \sum_{p \in P_d} \sum_{t \in T} \sum_{j \in \{1,2\} | j \neq i} \alpha_{pj} x_{ptj} + \sum_{p \in P_d \setminus \overline{P}} \sum_{t \in T \setminus \overline{T}} \alpha_{pi} x_{pti},$$

$$Y = \sum_{p \in \overline{P}} \sum_{t \in \overline{T}} \alpha_{pi} y_{pti}, a = \delta_i, b = v_d.$$

07.

The Hay bridge, shown in Fig. 11.23, differs from Maxwell's bridge by having a resistance R_1 in series with a standard capacitor C_1 instead of a parallel. For large phase angles, R_1 needs to be low; therefore, this bridge is more convenient for measuring high Q coils. For $Q = 10$, the error is 1% and for $Q = 50$ the error is 0.1%. Hence Hay's bridge is preferred for coils with a high Q and Maxwell's bridge for coils with a low Q.

Fig. 11.23 — Hay's Bridge

At balance $Z_1 Z_4 = Z_2 Z_3$, where

$Z_1 = R_1 - j/\omega C_1$

$Z_2 = R_2$

$Z_3 = R_3$

$Z_4 = R_4 + j\omega L_4$

Substituting these values in the balance equation we get

$$\left(R_1 - \frac{j}{\omega C_1}\right)(R_4 + j\omega L_4) = R_2 R_3$$

$$R_1 R_4 + \frac{L_4}{C_1} - \frac{jR_4}{\omega C_1} = R_2 R_3 + j\omega L_4 R_2$$

Equating the real and imaginary terms we have

$$R_1 R_4 + \frac{L_4}{C_1} = R_2 R_3 \qquad (11.15)$$

and $$\frac{R_4}{\omega C_1} = \omega L_4 R_2 \qquad (11.16)$$

Solving for L_4 and R_4 we have, $R_4 = \omega^2 L_4 C_1 R_2$

Substituting for R_4 in Eq. (11.16)

$$R_1 \omega^2 R_2 C_1 L_4 + \frac{L_4}{C_1} = R_2 R_3$$

Q.3	b)	Explain principle of operation and working of dual slope DVM. The dual slope integrating type DVM integrates the input voltage ViVi. The slope of the integrated signal is proportional to the input voltage under measurement. After certain period of time, say t1t1, the supply of input voltage ViVi is stopped, and a negative voltage -VrVr of the integrator is applied. Then the output signal of integrator experiences a negative slope, which is constant and proportional to the magnitude of the input voltage. The major blocks of a dual slope integrating type DVM are 1 An op-amp employed as an integrator 2 A level comparator 3. Oscillator for generating time pulses 4. Decimal counter 5. Block of logic circuitry Initially a pulse is applied to reset the counter and the output of flip-flop will be at logic '0.' The switch SrSr is in open condition and the switch SiSi is in closed condition. Now, the capacitor 'C' starts to charge. Once the output of the integrator becomes greater than zero, the output state of the comparator changes, which in turn opens the AND gate. When the gate opens, the output of the oscillator (clock pulses) are allowed to pass through it and are applied to the counter. Now the counter counts the number of pulses fed to it. As soon as it reaches its maximum count i.e. that is

where constraints (III.23) guarantee that a wavelength $t \in T$ is assigned to each lightpath defined in Y^*.

IV. Improvements

It is well-known that the derivation of strong formulations is of key importance to solve mixed integer linear programming problems using Branch and Cut (B&C) algorithms [18]. The linear programming (LP) relaxation of a problem is the problem considering the original formulation with the integer variables replaced by real variables (*i.e.*, obtained by replacing constraints (III.7) or (III.14) by $0 \leq y_{pti} \leq 1$). The performance of B&C depends on how close the fractional solutions of the LP relaxation are from the integer solutions of the original problem. Linear programming techniques able to cut off fractional solutions from the LP relaxation feasible set while maintaining all integer solutions of the original problem make the formulations stronger in the sense that B&C is able to find either an optimal solution in shorter runtime or a better solution for the same runtime limit. In this section, we describe two types of techniques to derive stronger formulations while keeping the total number of constraints of the model under control. The first type is the increase of the demand values. The second type is related with the addition of different constraints. These constraints are based on valid inequalities derived for simple mixed integer sets arising from relaxations of the original feasible set. We describe these improvements in detail in the following subsections.

A. Demand Values Increase

Since the cost of a solution depends only on the lightpaths and is not influenced on how occupied each lightpath is, we can increase the demand values provided that the required set of lightpaths remains unchanged. By increasing the demand values $v_d, d \in D$, we force the values of some x variables to increase, which forces the values of y variables also to increase in the LP relaxation (due to constraints (III.3) and (III.4) in Model 1 or (III.11) in Model 2). Note that the demand values increasing rule is parameter dependent. For $\delta_1 = 4$ and $\delta_2 = 10$, as considered in our problem instances, the possible values for the installed lightpaths capacity are the positive values given by all nonnegative integer linear combinations of 4 and 10, which are $4, 8, 10, 12, 14, 16, \ldots$. Hence, the demand values increasing rule is: for each $d \in D$, (i) we set $v_d = 4$ if $v_d < 4$, (ii) we set $v_d = 8$ if $4 < v_d < 8$ and (iii) we set $v_d = v_d + 1$ if $v_d > 8$ and odd.

B. Valid Inequalities

One possible approach to derive valid inequalities for a mixed integer linear problem is, first, to identify simple mixed integer sets arising as relaxations of the original feasible set. Consider the set of feasible solutions of Model 1 defined by X. In this section, we discuss three different relaxation sets of X for which valid inequalities are known. Using such inequalities, we derive valid inequalities for X.

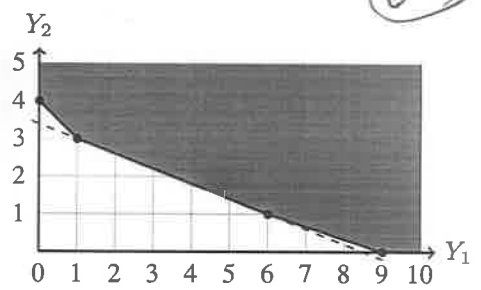

Fig. 1. Facet-defining inequalities for conv($\{(Y_1, Y_2) \in \mathbb{Z}^2 \mid 4Y_1 + 10Y_2 \geq 34\}, Y_1, Y_2 \geq 0$).

1) Integer Knapsack Relaxation: A first relaxation is obtained for each $d \in D$ from inequalities (III.2), (III.3) and (III.4) as follows:

$$\sum_{p \in P_d} \sum_{t \in T} (\delta_1 y_{pt1} + \delta_2 \alpha_p y_{pt2}) \geq \sum_{p \in P_d} \sum_{t \in T} (x_{pt1} + \alpha_p x_{pt2}) = v_d.$$

Setting $Y_1 = \sum_{p \in P_d} \sum_{t \in T} y_{pt1}$ and $Y_2 = \sum_{p \in P_d} \sum_{t \in T} \alpha_p y_{pt2}$, the previous inequality can be written as

$$\delta_1 Y_1 + \delta_2 Y_2 \geq v_d. \tag{IV.1}$$

Thus, the following two integer variables knapsack set is obtained as a relaxation of X.

$$X_{IK} = \left\{ (Y_1, Y_2) \in \mathbb{Z}^2 \mid \delta_1 Y_1 + \delta_2 Y_2 \geq v_d, Y_1, Y_2 \geq 0 \right\}.$$

The strongest valid inequalities for X_{IK} are the facet-defining inequalities which, for such sets, can be derived in polynomial time [19] and whose coefficients are obtained, in general, using the euclidian algorithm. The number of facet-defining inequalities is polynomial. For the particular case of coefficients considered in the computational results ($\delta_1 = 4$ and $\delta_2 = 10$), we have at most four non-trivial facet-defining inequalities for each $d \in D$ ($Y_1 \geq 0$ and $Y_2 \geq 0$ are called trivial), which are of the following forms: $2Y_1 + 5Y_2 \geq \left\lfloor \frac{v_d}{2} \right\rfloor + 1$, $Y_1 + 3Y_2 \geq \left\lfloor \frac{v_d}{4} \right\rfloor + 1$, $Y_1 + 2Y_2 \geq \left\lfloor \frac{v_d}{5} \right\rfloor + 1$ and $Y_1 + Y_2 \geq \left\lfloor \frac{v_d}{10} \right\rfloor + 1$ leading to the following valid inequalities for X:

$$2 \sum_{p \in P_d} \sum_{t \in T} y_{pt1} + 5 \sum_{p \in P_d} \sum_{t \in T} \alpha_p y_{pt2} \geq \left\lfloor \frac{v_d}{2} \right\rfloor + 1,$$

$$\sum_{p \in P_d} \sum_{t \in T} y_{pt1} + 3 \sum_{p \in P_d} \sum_{t \in T} \alpha_p y_{pt2} \geq \left\lfloor \frac{v_d}{4} \right\rfloor + 1,$$

$$\sum_{p \in P_d} \sum_{t \in T} y_{pt1} + 2 \sum_{p \in P_d} \sum_{t \in T} \alpha_p y_{pt2} \geq \left\lfloor \frac{v_d}{5} \right\rfloor + 1,$$

$$\sum_{p \in P_d} \sum_{t \in T} y_{pt1} + \sum_{p \in P_d} \sum_{t \in T} \alpha_p y_{pt2} \geq \left\lfloor \frac{v_d}{10} \right\rfloor + 1.$$

Example 3: Let $v_d = 34$, for some $d \in D$. So $X_{IK} = \{(Y_1, Y_2) \in \mathbb{Z}^2 \mid 4Y_1 + 10Y_2 \geq 34, Y_1, Y_2 \geq 0\}$. The segment line $4Y_1 + 10Y_2 = 34$ is drawn by dashed line in Fig. 1. As it is shown in Fig. 1, the convex hull of X_{IK} has three non-trivial facet-defining inequalities: $2Y_1 + 5Y_2 \geq 17$, $Y_1 + 3Y_2 \geq 9$, and $Y_1 + Y_2 \geq 4$. Note that, for $v_d = 34$, one of the inequalities described above is not facet-defining and, therefore, do not need to be considered.

the counter is preset to run for a time period r: in this condition the maximum count will be'9999', and for the next immediate clock pulse the count changes or goes to '0000' and the flip-flop will be activated.

Therefore, the output of flip flop becomes logic 'l' which in turn activates the switch drive circuitry. This makes the switch SiSi to open and SrSr to close (i.e. the supply of ViVi will be stopped, and the supply of V is applied to the integrator.) With this applied signal the output of the integrator will be a constant negative slope i.e. its output signal linearly decreases to zero. This again makes the output of the comparator to change its state which in turn closes the gate.

Here, the discharging time t2t2 of the capacitor is proportional to the input voltage signal Vi. During this discharging period the counter indicates the count. As soon as, the negative slope reaches zero volts the comparator changes its output state to 'zero' which in turn locks the gate. Once the output of integrator becomes zero (or the input of the comparator is zero) the counter will be stopped and the counted pulses are displayed (which directly gives the input voltage).

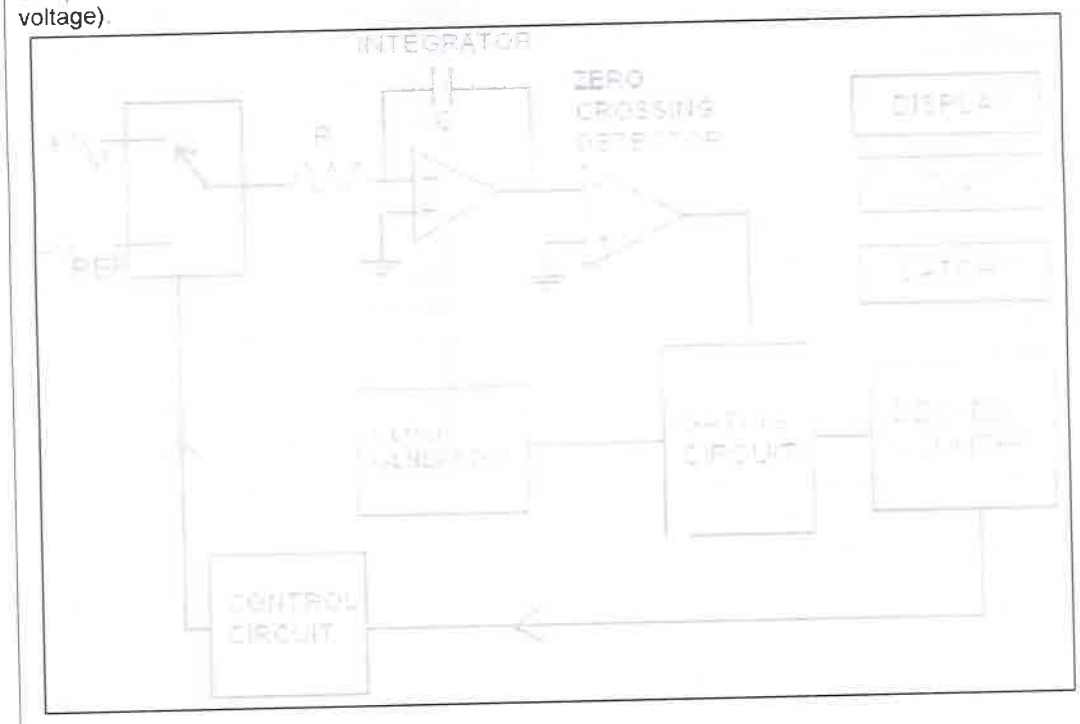

Figure - Block Diagram of Dual Slope DVM

Q.4 a) Define power and energy and explain working of a single phase energy meter.

Power is the rate at which energy is supplied (or energy per unit time). Power is measured in watts. One watt is equal to one joule supplied per second. It is the flow of energy at any one time and is measured in Watts. Equipment and appliances are rated on a basis of Watts, and the amount of energy generated by equipment, or the amount consumed by equipment and appliances is measured in Watt-hours.

Energy –

Energy is referred to as the ability to do work. Energy is measured in units called joules, J, or in watt hours as shown below. One kilojoule, kJ is equal to a thousand joules, and one mega joule, MJ, is equal to a million joules. Watt hours (Wh), are a convenient way of measuring electrical energy. One watt-hour is equal to a constant one watt supply of power supplied over one hour (3600 seconds). If a bulb is rated at 40watts, in one hour it will use 40 Wh, and in 8 hours it will use 320 Wh of energy.

Working of an Energy Meter –

- An electric meter or energy meter is a device that measures the amount of electrical energy supplied to or produced by a residence, business or machine.
- Modern electricity meters operate by continuously measuring the instantaneous voltage (volts) and current (amperes) and finding the product of these to give instantaneous electrical power (watts), which is then integrated against time to give energy used (joules, kilowatt-hours etc).
- The meters fall into two basic categories, electromechanical and electronic.

lightpaths have enough capacity to groom their supported client demands. Constraints (III.5) ensure that, on each fiber e, each wavelength t is assigned to at most one lightpath. Constraints (III.6) and (III.7) are the variable domain constraints.

Alternatively, consider variables x_{pt} representing the demand that is routed through path $p \in P$ in the solution with the assigned wavelength $t \in T$, i.e.:

$$x_{pt} = \sum_{i=1}^{2} x_{pti}, \tag{III.8}$$

With these new variables, the GRWA network design problem can be formulated as:

$$min \sum_{p\in P}\sum_{t\in T}\sum_{i=1}^{2} c_{pi} y_{pti}, \tag{III.9}$$

$$s.t. \sum_{p\in P_d}\sum_{t\in T} x_{pt} = v_d, \quad d \in D, \tag{III.10}$$

$$x_{pt} \le \delta_1 y_{pt1} + \alpha_p \delta_2 y_{pt2}, \quad p \in P,\ t \in T, \tag{III.11}$$

$$\sum_{p\in P_e}\sum_{i=1}^{2} y_{pti} \le 1, \quad e \in E,\ t \in T, \tag{III.12}$$

$$x_{pt} \ge 0, \quad p \in P,\ t \in T, \tag{III.13}$$

$$y_{pti} \in \{0,1\}, \quad p \in P,\ t \in T,\ i \in \{1,2\}. \tag{III.14}$$

Henceforward we consider the following two mixed integer linear programming models: Model 1 defined by (III.1)–(III.7) and Model 2 defined by (III.9)–(III.14). In terms of complexity, the number of constraints is $\mathcal{O}(\max\{|D|, |P|\cdot|T|\})$ and the number of variables is $\mathcal{O}(|P|\cdot|T|)$ in both models. In the general case, $|P|$ increases exponentially with the graph size but in our case the transparent reach of the lightpaths keeps this number within reasonable values for relevant sized graphs. Next, we provide two important remarks.

Remark 1: Constraints (III.11) *are obtained by summing up constraints* (III.3) *and* (III.4)*, and applying* (III.8)*. Thus, relating the two models by summing up variables x_{pti}, $i \in \{1,2\}$, and adding constraints* (III.8) *to the second model, one can easily check that the aggregated Model 2 is weaker than Model 1, in the sense that the projection of its linear relaxation set contains the linear relaxation of constraints* (III.2)–(III.7)*. However, since the x variables do not appear in the objective function one can also check that the linear relaxation of both models provides the same lower bound.*

Remark 2: One can check that the matrix of coefficients of x variables is totally unimodular in both models, that is, each square submatrix of the matrix of coefficients has determinant $0, -1$, or $+1$. Therefore, for each binary set of values for the y variables the linear relaxation of the resulting feasible set will always provide integer values for x variables, see [18] for details. Hence, we can drop the integrality requirements on x variables in both models, as defined in constraints (III.6) *and* (III.13)*.*

Based on these two remarks, we might expect that Model 2 is better than Model 1 since it has slightly less number of constraints and half of the real variables although the number of integer variables remains the same. Nevertheless, with the improvements described in the next section, the computational results show that the resulting methods based on Model 1 obtain solutions with lower cost values.

Note that, when removing constraints (III.5) on Model 1 and maintaining the integrality of the y_{pti} variables, the problem becomes easy to solve since it can be separated in a set of subproblems, one for each $d \in D$. This is an easy way to determine valid lower bounds that will be used in the computational results. Assuming that $c_{pi} = c_i$, for all $p \in P$ (since in a transparent network regenerators are not used), the subproblem associated with demand pair $d \in D$ becomes a 2-dimensional knapsack problem defined as:

$$\min\{c_1 Y_1 + c_2 Y_2 : \delta_1 Y_1 + \delta_2 Y_2 \ge v_d, Y_1, Y_2 \in \mathbb{Z}_+\},$$

where $Y_1 = \sum_{p\in P_d}\sum_{t\in T} y_{pt1}$ and $Y_2 = \sum_{p\in P_d}\sum_{t\in T} \alpha_p y_{pt2}$. This subproblem can be efficiently solved by an algorithm based on the Euclidean algorithm (see [19] for details).

The overall problem can be decomposed in different ways and many works use different decompositions to derive solution techniques. The one used in [14] decomposes the problem in the Grooming and Routing (GR) problem and the Wavelength Assignment (WA) problem. Since the method of [14] will be used in the computational results, we formally define this decomposition. The GR problem is modeled as:

$$min \sum_{p\in P}\sum_{i=1}^{2} c_{pi} Y_{pi}, \tag{III.15}$$

$$s.t. \sum_{p\in P_d}\sum_{i=1}^{2} X_{pi} = v_d, \quad d \in D, \tag{III.16}$$

$$X_{p1} \le \delta_1 Y_{p1}, \quad p \in P, \tag{III.17}$$

$$X_{p2} \le \alpha_p \delta_2 Y_{p2}, \quad p \in P, \tag{III.18}$$

$$\sum_{p\in P_e}\sum_{i=1}^{2} Y_{pi} \le K, \quad e \in E, \tag{III.19}$$

$$X_{pi} \ge 0, \quad p \in P,\ i \in \{1,2\}, \tag{III.20}$$

$$Y_{pi} \in \{0,1\}, \quad p \in P,\ i \in \{1,2\}, \tag{III.21}$$

where $K = |T|$, $X_{pi} = \sum_{t=1}^{K} x_{pti}$ and $Y_{pi} = \sum_{t=1}^{K} y_{pti}$. The new variables are aggregated versions of the original ones and GR assigns a routing path to each lightpath ensuring that the fiber capacities are not exceeded. The WA subproblem determines a wavelength assignment to the lightpaths of the GR solution. In order to define an objective function to WA, we use the minimization of the number of used wavelengths. Let w_t be a binary variable indicating whether wavelength t is used or not. Given a solution (X^*, Y^*) of GR, the WA problem is modeled as:

$$min \sum_{t\in T} w_t, \tag{III.22}$$

$$s.t. \sum_{t\in T} y_{pti} = Y^*_{pi}, \quad d \in D,\ p \in P_d,\ i \in \{1,2\}, \tag{III.23}$$

$$y_{pti} \le w_t, \quad p \in P,\ t \in T,\ i \in \{1,2\}, \tag{III.24}$$

$$w_t \le w_{t-1}, \quad t \in T,\ t > 1, \tag{III.25}$$

$$w_t \in \{0,1\}, \quad t \in T, \tag{III.26}$$

(III.7),

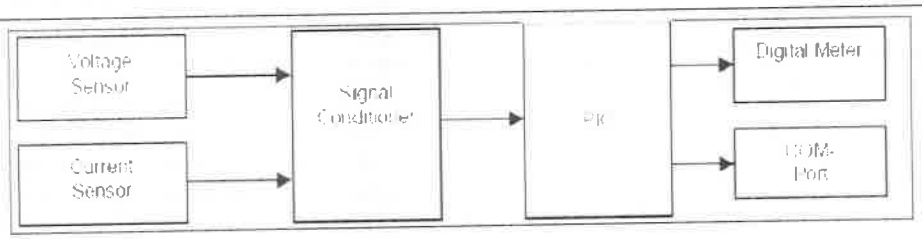

Figure 2 - A basic Energy Meter

Q.4 b) Draw and explain capacitive transducer for level measurement

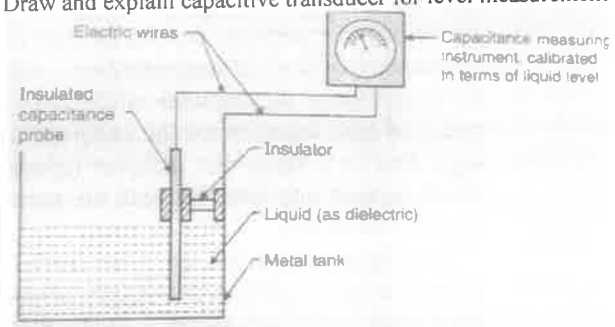

It consists of an insulated capacitance probe which is the metal fixed near and parallel to the metal wall of the tank.The metal rod of the electrode acts as one plate of the capacitor and the tank wall acts as the other plate.

It is based on capacitance equation,

$$C = \frac{\in A}{D}$$

Where, C = Capacitance in farad

$\in$ = Dielectric constant

A = Area of plate in m^2

D = Distance between two plates in m

If A and D are constant, $C \propto \in$.

As level rises. the air or gas normally surrounding the electrode is displaced by material having a different dielectric constant. A change in the value of the capacitor takes place because the dielectric between the plates has changed.

When level of liquidin thetank rises. thecapacitanceincreases. when liquid level ofthe tank decreases, the capacitance also decreases. This increase and decrease in the capacitance is measured and is displayed on indicator calibrated in terms of liquid level.

Q.5 a) Draw the block diagram of generalised measurement system and explain its component

The generalized measurement system consists of three main functional elements. They are:

1. **Primary sensing element,** which senses the quantity under measurement
2. **Variable conversion element,** which modifies suitably the output of the primary sensing element, and
3. **Data presentation element** that renders the indication on a calibrated scale

The block diagram is shown below. Detailed descriptions of each block are as follows

longer transparent reach values for each lightpath if wavelengths are assigned on each fiber minimizing the interference between them. In [6], this problem is addressed showing that efficient ILP models to define such problem are quite hard. In [7], the authors propose ILP models, for small and medium sized transparent networks and, since the models are hard to solve larger networks, a three-phase heuristic is proposed. In [8], the authors propose a heuristic where the RWA problem is decomposed into its routing and wavelength assignment subproblems which are solved separately. Nevertheless, the transparent reach gains, while considering the impairment aware variant, are only possible with lightly loaded networks where only a few wavelengths are required on each fiber. When total demand is significant, most of the wavelengths have to be used in all fibers and the transparent reach of each lightpath becomes a conservative value independent of the wavelengths assigned to the other lightpaths.

The GRWA problem, which is much harder than the classical RWA problem, has been also addressed in recent works. In [9], an additional constraint is considered on the maximum number of transceivers on each node and the objective is the throughput maximization (it is assumed that the network cannot accommodate the total required demand). The authors propose a path-based formulation and, since computational results show that only small network sizes can be dealt with, they propose a heuristic based on column generation techniques. In [10], the GRWA network design problem is addressed considering the minimization of the number of lightpaths. They solve to optimality a test instance with 6 nodes with a fiber capacity of up to 30 wavelengths (still significantly lower than the capacity of current optical networks). For bigger instances, they propose the decomposition of the problem in two subproblems (Grooming problem + RWA problem) that are solved sequentially. For heavily loaded networks, though, this decomposition might fail since the solution of the grooming problem might be unfeasible to the RWA problem. Some works ([11], [12]) use path based formulations and branch-and-price as a solution technique but also do not consider the wavelength continuity constraints. Other works use a reduced set of candidate paths ([11], [13]) to make the methods scalable for larger problem instances. This approach will be compared with our approach in Section VI.

All these previous works dealing with the GRWA problem consider that all lightpaths are of the same line rate. In [14], though, the authors deal with the mixed line rates case. They propose the decomposition of the problem in the Grooming and Routing (GR) subproblem and the Wavelength Assignment (WA) subproblem that are solved sequentially. They start by solving the two subproblems considering a fiber capacity of T wavelengths. If the solution of GR makes the WA unfeasible, they decrement T and repeat the process. This approach will be compared with our approach in Section VI.

As a final remark, note that network design problems fall in the category of static (G)RWA problems. On the other hand, dynamic problems consider that demand requests arrive randomly, one at a time, and last in the network a finite random time. In this case, the aim is to optimize some performance metric like blocking probability (see [15]–[17]).

III. Mixed Integer Linear Programming Models

Consider a fiber network defined by the graph $G = (N, E)$ such that the spectrum of each fiber $e \in E$ is organized in a set T of $|T|$ wavelengths. Consider a set of demand pairs D such that each demand pair $d \in D$ is a node pair that has at least one client demand between them. So, a demand pair $d \in D$ is defined by a pair of end nodes in G and an integer demand value v_d with the aggregated number of client demand interfaces that must be supported between its end nodes. To support the demands of each $d \in D$, consider two types of lightpaths (type 1 and 2) that can be set on the fiber network, defined by their capacities δ_1 and δ_2 (in number of client demand interfaces), respectively, such that $\delta_1 < \delta_2$. Since we consider single hop grooming, the end nodes of each lightpath are the end nodes of the demand pair supported by it (note that different lightpaths supporting the client demand interfaces between the same end nodes can be routed differently).

Each lightpath can be set in the underlying fiber network through a routing path whose length cannot be higher than its transparent reach and lightpaths with higher line rates have lower transparent reach values. So, the transparent reach l_1 of a lightpath of type 1 is higher than the transparent reach l_2 of a lightpath of type 2. Consider P_d as the set of all routing paths for lightpaths of type 1 between the end nodes of demand pair $d \in D$ whose total length is not higher than l_1. For each routing path $p \in P_d$, the binary parameter α_p is one if the total length of p is also not higher than l_2. A lightpath of type $i \in \{1, 2\}$ routed in path $p \in P_d$ between the end nodes of $d \in D$ has an associated cost of c_{pi}, such that $c_{p1} < c_{p2}$. Additionally, consider the set $P = \bigcup_{d \in D} P_d$ of all routing paths and, from this set, the subsets P_e as the sets of all routing paths that include fiber $e \in E$.

Consider the following variables. Variable x_{pti} indicates the amount of demand routed through path $p \in P$ with the assigned wavelength $t \in T$ and using a lightpath of type $i \in \{1, 2\}$. Binary variable y_{pti} takes the value 1 if path $p \in P$ is in the solution with the assigned wavelength $t \in T$ as a lightpath of type $i \in \{1, 2\}$ (it takes value 0, otherwise). The GRWA network design problem can be formulated as:

$$min \sum_{p \in P} \sum_{t \in T} \sum_{i=1}^{2} c_{pi} y_{pti}, \tag{III.1}$$

$$s.t. \sum_{p \in P_d} \sum_{t \in T} \sum_{i=1}^{2} x_{pti} = v_d, \quad d \in D, \tag{III.2}$$

$$x_{pt1} \leq \delta_1 y_{pt1}, \quad p \in P,\ t \in T, \tag{III.3}$$

$$x_{pt2} \leq \alpha_p \delta_2 y_{pt2}, \quad p \in P,\ t \in T, \tag{III.4}$$

$$\sum_{p \in P_e} \sum_{i=1}^{2} y_{pti} \leq 1, \quad e \in E,\ t \in T, \tag{III.5}$$

$$x_{pti} \geq 0, \quad p \in P,\ t \in T,\ i \in \{1, 2\}, \tag{III.6}$$

$$y_{pti} \in \{0, 1\}, \quad p \in P,\ t \in T,\ i \in \{1, 2\}. \tag{III.7}$$

The objective function (III.1) is to minimize the solution cost, which is the sum of the lightpath costs. Constraints (III.2) guarantee that all client demands are routed through lightpaths. Constraints (III.3) and (III.4) guarantee that the selected

13

Primary Sensing Element - The measurement first comes into contact with primary sensing element where the conversion takes place. This is done by a transducer which converts the measured quantity into a usable electrical output. The transduction may be from mechanical, electrical, optical to any related form.

Variable Conversion Element - The output of the primary sensing element is in the electrical form suitable for control, recording and display. For the instrument to perform the desired function, it may be necessary to convert this output to some other suitable for preserving the original information. This function is performed by the variable conversion element. A system may require one or more variable conversion suitable to it.

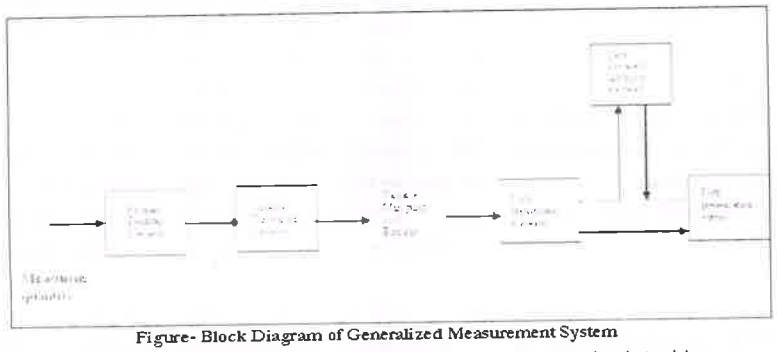

Figure- Block Diagram of Generalized Measurement System

Variable Manipulation Element - The signal gets manipulated here preserving the original nature of it. For example, an amplifier accepts a small voltage signal as input and produces a voltage, of greater magnitude. The output is the same voltage but of higher value, acting as a voltage amplifier. Here the voltage amplifier acts as a variable manipulation element since it amplifies the voltage. The element that follows the primary sensing element in a measurement system is called signal conditioning element. Here the variable conversion element and variable manipulation element are collectively called as Data Conditioning Element or Signal Conditioning Element.

Data Transmission Element - The transmission of data from one another is done by the data transmission element. In case of spacecraft, the control signals are sent from the control stations by using radio signals.

The stage that follows the signal conditioning element and data transmission element collectively is called the intermediate stage.

Data Presentation Element - The display or readout devices which display the required information about the measurement, forms the data presentation element. Here the information of the measured has to be conveyed for, monitoring, control or analysis purposes. In case of data to be monitored, visual display devices are needed like ammeters and voltmeters. In case of data to be recorded, recorders like magnetic tapes, T.V equipment, and storage type CRT, printers, and so on are used.

Q.5	b)	Draw andexplain Wheatstone bridge and derive expression for measurement of resistance. or measuring any electrical resistance accurately, Wheatstone bridge is widely used. There are two known resistors - one variable resistor and one unknown resistor connected in bridge form as shown below. By adjusting the variable resistor, the current through the Galvanometer is made zero. When the current through the galvanometer becomes zero, the ratio of two known resistors is exactly equal to the ratio of adjusted value of variable resistance and the value of unknown resistance. In this way, the value of unknown electrical resistance can easily be measured by using a Wheatstone Bridge. **Working –** The general arrangement of Wheatstone bridge circuit is shown in the figure below. It is a four arms bridge circuit where arm AB, BC, CD and AD are consisting of electrical resistances P, Q, S and R respectively. Among these resistances P and Q are known fixed electrical resistances and these two arms are referred as ratio arms. An accurate and sensitive Galvanometer is connected between the terminals B and D through a switch S2S2. The voltage source of this Wheatstone bridge is connected to the terminals A and C via a switch S1S1 as shown. A variable resistor S is connected between point C and D.

approximately 10 Gbps (in this case, there is no grooming), (ii) four such interfaces can be groomed into a lightpath of type OTU-3 with a line rate of approximately 40 Gbps or (iii) ten such interfaces can be groomed into a lightpath of type OTU-4 with a line rate of approximately 100 Gbps.

Each lightpath alternative has its own associated cost and transparent reach and, in practice, lightpaths of higher line rates can groom more client demands at the cost of being more expensive and having shorter transparent reach. The Grooming, Routing and Wavelength Assignment (GRWA) network design problem is the combination of the grooming problem with the classical RWA problem and consists in assigning routing paths and wavelengths for a minimum cost set of lightpaths able to groom all client demands.

In general, we can distinguish two grooming types: single hop and multi hop grooming. In single hop grooming, lightpaths groom only client demands between their end nodes. In multi hop grooming, a client demand can be groomed with some other demands into a lightpath from its source node to an intermediate node and groomed again with other demands from the intermediate node to its destination node (this is the two hop grooming case but the idea can be generalized to multiple hops). Although some gains can be achieved with lightly loaded networks, these gains become marginal for reasonably loaded networks (most lightpaths become fully occupied with direct demands) and, since it makes network management more complex, network operators usually resort to single hop grooming only.

We address the GRWA network design problem in the context of a network operator with a highly loaded network based on lightpaths of a given OTU type who aims to upgrade it by introducing lightpaths of the next higher line rate OTU type. Such lightpaths enable it to support more client demands preventing the network to become fully occupied. So, the operator aims to compute the lowest cost set of lightpaths able to groom all its client demands allowing lightpaths of the two OTU types to coexist on its network. The GRWA network design problem addressed in this paper considers a transparent optical network, single hop grooming, client demands of a single interface type and lightpaths of two line rates.

Since GRWA (and, also, RWA) is NP-hard, most previous works addressing these problems either propose pure heuristic approaches or decompose the problem into subproblems (grooming problem + routing problem + wavelength assignment problem) and solve them sequentially. Although the decomposition approach can be exact when the network is lightly loaded (in this case, the grooming optimal solution can be computed separately since there is always a RWA solution for any grooming configuration), this is not our case of interest. Some works (reviewed in the next section) have proposed integer linear programming formulations for the classical RWA problem and, more recently, for the harder GRWA problem but the reported results have shown so far that they can deal with problem instances significantly smaller than the real cases. Nevertheless, using advanced integer linear programming modeling techniques, together with the huge increase of computer CPU processing capacity (multiple core CPUs and multi-thread solver packages) and RAM memory capacity, we can now aim to use integer linear programming to deal with real sized problem instances.

In this paper, we first discuss two slightly different mixed integer linear programming models that define the GRWA network design problem. Then, we improve them with strengthening techniques (one based on increasing some problem parameters and the others based on three types of additional constraints) that, when applied to the previous models, make their linear relaxation solutions closer to the integer solutions. Finally, we use the resulting models to derive a hybrid heuristic method which combines a relax-and-fix approach with an integer linear programming based local search approach. We present computational results showing that this heuristic is able to find solutions with a cost value very close to the optimal one. Moreover, when compared with previous approaches (used in problem variants close to the one addressed here), the proposed heuristic is shown to compute solutions, on average, with better cost values and/or in shorter runtimes.

This paper is organized as follows. Section II presents the previously published related work. Section III discusses the two formulations defining our GRWA problem variant, together with a method to compute valid lower bounds and a decomposition that is used by other works. Section IV describes the different techniques used to strengthen the previous formulations. Section V presents the hybrid heuristic. The computational results are described and discussed in Section VI. Finally, Section VII presents the main conclusions.

II. Related Work

The classical RWA problem is known to be NP-hard [1]. It has been extensively studied in the literature although only some of the works have dealt with efficient integer linear programming formulations for it. In [2], Integer Linear Programming (ILP) models are proposed for the RWA problem assuming that wavelength conversion is available on network nodes (a problem variant that makes the problem tractability much easier) and the aim is to minimize the average number of demand routing hops. In [3], different ILP models for the RWA network design problem are compared (a flow based formulation and a source based formulation) addressing both cases with or without wavelength conversion. Nevertheless, the computational results reported in both works ([2], [3]) show that only problem instances with a fiber capacity up to 10 wavelengths can be solved to optimality. Finally, in [4], different path-based formulations are compared to solve the RWA problem aiming to maximize the total number of established lightpaths. They show that branch-and-price methods can solve the problem more efficiently than using compact models (*i.e.*, models with a polynomial number of variables) and the computational results show that near optimal solutions can be obtained for relevant sized networks with fiber capacity of up to 34 wavelengths. A similar approach was also proposed in [5] with more modest computational results, also due to the computational resources available by then.

A more recent variant of the RWA problem, known as impairment aware RWA (IA-RWA), considers the interference between lightpaths due to non-linear impairments: we can get

157

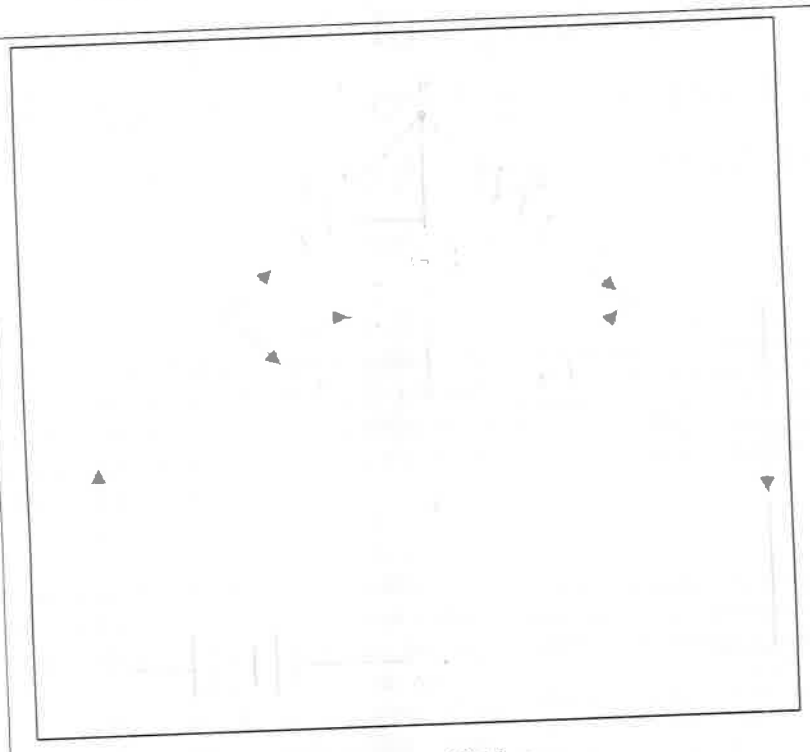

Wheastone Bridge

The potential at point D can be varied by adjusting the value of variable resistor. Suppose current I1I1 and current I(2)I(2)are flowing through the paths ABC and ADC respectively.
If we vary the electrical resistance value of arm CD the value of current I2I2 will also be varied as the voltage across A and C is fixed. If we continue to adjust the variable resistance one situation may come when voltage drop across the resistor S that is I2I2.S, which is exactly equal to voltage drop across resistor Q that is I1I1.Q
Thus the potential at point B becomes equal to the potential at point D hence potential difference between these two points is zero, hence, current through galvanometer is nil. Then the deflection in the galvanometer is nil when the switch S2S2 is closed.
Now, from Wheatstone bridge circuit, we get

And

Current I2=VR+SI2=VR+S

Now potential of point B in respect of point C is nothing but the voltage drops across the resistor Q and this is

I1Q=V.QP+QI1Q=V.QP+Q----------(i)

Again potential of point D in respect of point C is nothing but the voltage drops across the resistor S and this is

I1Q=V.SR+SI1Q=V.SR+S----------(ii)

Equating equations (i) and (ii) we get,

V.QV+Q=V.SR+S->QP+Q=SR+SV.QV+Q=V.SR+S->QP+Q=SR+S

-->P+QQ=R+SS->PQ+1=RS+1->PQ=RS->P+QQ=R+SS->PQ+1=RS+1->PQ=RS

-->R=S.PQ->R=S×PQ

Q.6	a)	Explain dual slope ADC with neat block diagram and comment on its speed The dual-slope integration type of A/D conversion is a very popular method for digital voltmeter applications. When compared to other types of ADC techniques, the dual-slope method is slow but is quite adequate for a digital voltmeter used for laboratory measurements.

The Minimum Cost Design of Transparent Optical Networks Combining Grooming, Routing, and Wavelength Assignment

Agostinho Agra, Amaro de Sousa, and Mahdi Doostmohammadi

Abstract— **As client demands grow, optical network operators are required to introduce lightpaths of higher line rates in order to groom more demand into their network capacity. For a given fiber network and a given set of client demands, the minimum cost network design is the task of assigning routing paths and wavelengths for a minimum cost set of lightpaths able to groom all client demands. The variant of the optical network design problem addressed in this paper considers a transparent optical network, single hop grooming, client demands of a single interface type, and lightpaths of two line rates. We discuss two slightly different mixed integer linear programming models that define the network design problem combining grooming, routing, and wavelength assignment. Then, we propose a parameters increase rule and three types of additional constraints that, when applied to the previous models, make their linear relaxation solutions closer to the integer solutions. Finally, we use the resulting models to derive a hybrid heuristic method, which combines a relax-and-fix approach with an integer linear programming-based local search approach. We present the computational results showing that the proposed heuristic method is able to find solutions with cost values very close to the optimal ones for a real nation-wide network and considering a realistic fiber link capacity of 80 wavelengths. Moreover, when compared with other approaches used in the problem variants close to the one addressed here, our heuristic is shown to compute solutions, on average, with better cost values and/or in shorter runtimes.**

Index Terms— **Optical transport networks, grooming, routing and wavelength assignment, mixed integer linear programming, valid inequalities, hybrid heuristics.**

I. Introduction

CONSIDER a transparent optical network composed by a set of optical switching nodes and a set of fibers, each one connecting a pair of nodes. In modern fixed grid networks, the spectrum of each fiber is organized in a set T of $|T|$ different wavelengths of 50 GHz spectrum width where, typically, $|T| = 80$. Data is transmitted from its source node to its destination node by lightpaths which are optical paths crossing a set of fibers and using one wavelength on each fiber. In a transparent optical network, a lightpath must be assigned with the same wavelength on all fibers of its path. For a given set of lightpaths to be established on a given fiber network, the classical Routing and Wavelength Assignment (RWA) problem consists in assigning a routing path and a wavelength for each lightpath, aiming to optimize a given target objective.

Since data is in the electrical domain and lightpaths are in the optical domain, a pair of electrical-optical converters, named transponders, is placed on the end nodes of each lightpath. Moreover, the optical signal propagation is affected by different factors like attenuation, dispersion, crosstalk and other non-linear factors, commonly named physical impairments, which limit the maximum length the signal can be propagated from transmitter to receiver. To work properly, a lightpath has an associated maximum length, commonly named transparent reach. If a lightpath is required on a path whose length is higher than its transparent reach, regenerators must be placed at one or more intermediated nodes of the lightpath (a regenerator is a back-to-back pair of transponders that recovers the optical signal into the electrical domain and resends it back to the optical domain). Nevertheless, the use of regenerators is expensive and puts an additional burden on the network management and, therefore, they are avoided when possible (when regenerators are used, the network is referred to as a translucent network).

Modern optical networks allow the client demands to be groomed on lightpaths, *i.e.*, multiple client demands grouped to be transmitted over a single lightpath. This has two benefits: it reduces the required number of lightpaths and it enlarges the total transmission capacity of the network. In this case, the transponders at the end nodes of a lightpath have one multiplexer coupled to each of them (a transponder coupled with a multiplexer is named a muxponder). The Optical Transport Network (OTN) ITU-T G.709 recommendation defines the grooming alternatives and resulting line rates for different types of client demand interfaces. In this recommendation, grooming is implemented in an electrical layer, named Optical Transport Unit (OTU), and there are different OTU types to support different client interface types. For example, for client interfaces of 10 Gbps Ethernet type: (i) one such interface can be transmitted in a lightpath of type OTU-2 with a line rate of

Manuscript received December 30, 2014; revised August 14, 2015 and February 3, 2016; accepted March 8, 2016; approved by IEEE/ACM TRANSACTIONS ON NETWORKING Editor D. Medhi. The work of A. Agra and M. Doostmohammadi was supported by the Fundação para a Ciência e a Tecnologia under Grant UID/MAT/04106/2013 and the program COMPETE: FCOMP-01-0124-FEDER-041898 under Grant EXPL/MATNAN/1761/2013. The work of A. de Sousa was supported under Grant UID/EEA/50008/2013 and the Project "Cptimizing Next-generation Elastic Core Network Infrastructure" under Grant PTDC/EEITEL/3303/2012.

A. Agra is with the Centro de Investigação e Desenvolvimento em Matemática e Aplicações (CIDMA), Departamento de Matemática, Universidade de Aveiro, Aveiro 3810-193, Portugal (e-mail: aagra@ua.pt).

A. de Sousa is with the Instituto de Telecomunicações/DETI, Universidade de Aveiro, 3810-193 Aveiro, Portugal (e-mail: asou@ua.pt).

M. Doostmohammadi is with the Centro de Investigação e Desenvolvimento em Matemática e Aplicações (CIDMA), Departamento de Matemática, Universidade de Aveiro, Aveiro 3810-193, Portugal, and also with the Instituto de Engenharia Mecânica (IDMEC), Instituto Superior Técnico, University of Lisbon, Lisbon 1649-004, Portugal (e-mail: mahdi@ua.pt).

Digital Object Identifier 10.1109/TNET.2016.2544760

17

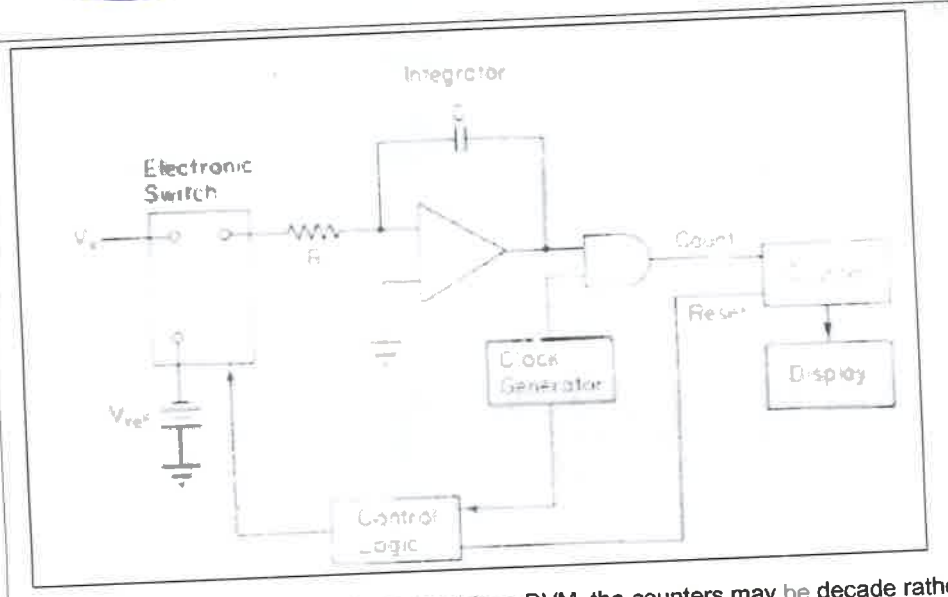

When a dual-slope A/D converter is used for a DVM, the counters may be decade rather than binary and the segment and digit drivers may be contained in the chip. When the converter is to be interfaced to a microprocessor, and many high performance DVMs use microprocessors for data manipulation, the counters employed are binary.

Working -

In the dual-slope technique, an integrator is used to integrate an accurate voltage reference for a fixed period of time. The same integrator is then used to integrate with the reverse slope, the input voltage, and the time required to return to the starting voltage is measured. The order of integrations does not matter. Consider the integration circuit shown in the figure.

Where 't' is the elapsed time from when the integration began. The above Equation also assumes that the integrator capacitor started with no charge & thus the output of the integrator started at zero volts

Q.6 b) Define Q factor and explain working of a Q meter for Q factor measurement.

The quality factor or Q-factor of a resonant circuit is a measure of the "goodness" or quality of a resonant circuit. A higher value for this figure of merit corresponds to a narrower bandwidth, which is desirable in many applications. Q is the ratio of power stored to power dissipated in the circuit reactance and resistance

A practical application of "Q" is that voltage across L or C in a series resonant circuit is Q times total applied voltage. In a parallel resonant circuit, current through L or C is Q times the total applied current.

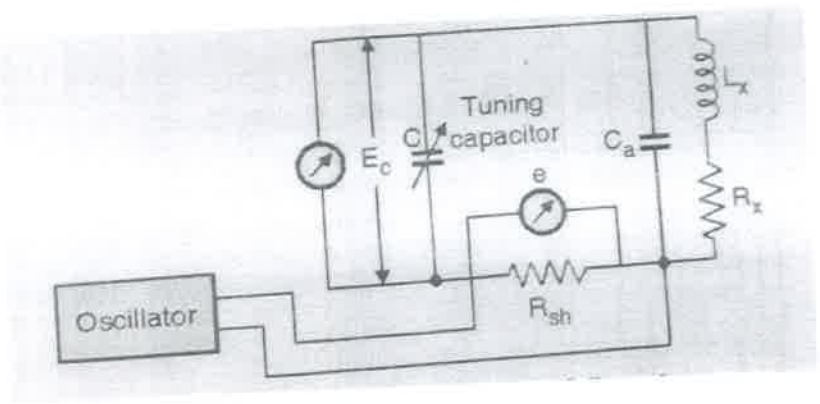

The Q-meter is an instrument designed for the measurement of Q-factor of the coil as well as for the measurement of electrical

Computational intelligence in Robotics and Automation July 16-20,2003, Kobe, Japan.

13 E.H.Zhang, B. Jiang, J. H. Duan, Z. Z. Bian," Research on Paper Currency Recognition by Neural Networks", Proceedings of the 2nd Int. Conference on Machine Learning and Cybernetics, 2003

14 Jae-Kang Lee and Hwan Kim,"New Recognition Algorithm for Various Kinds of Euro Banknotes" 0-7803-7906-3/03/ 2003 IEEE.

15 F.H Kong, J.Quab Ma , J.FengLiu,"Paper Currency Recognition Using Gaussian Mixture Models based on Structural Risk Minimization" Proceedings of the Fifth International Conference on Machine Learning and Cybernetics, Dalian, 13-16 August 2006.

16 Ji Qian,DongpingQian,MengjieZhang,"A Digit Recognition System for Paper Currency Identification Based on Virtual Instruments"1-4244-0555-6/06 © 2006 IEEE.

properties of coils and capacitors.

This instrument operates on the principle of series resonance i.e. at resonate condition of an AC series circuit voltage across the capacitor is equal to the applied voltage times of Q of the circuit. If the voltage applied across the circuit is kept constant. then voltmeter connected across the capacitor can be calibrated to indicate Q directly.

The fake currency detection using image processing was implemented on MATLAB. Features of currency note like serial number, security thread, Identification mark, Mahatma Gandhi portrait were extracted .The process starts from image acquisition to calculation of intensity of each extracted feature. The systemis capable of extracting features even if the note has scribbles on it. The algorithm processed here works suitably for the newly introduced 500 and 2000denomination.. Hardware implementation of the proposed system can also be done using suitable processor so that to increase the speed of detection. An automatic railway ticket booking system can also be proposed which includes currency detection as one of its part.

Other techniques: The best anti counterfeit device we can buy for the money is an Ultraviolet counterfeit detection scanner. Best used in highly lit point of sale locations, the UV detector identifies the ultraviolet security features present in most currencies. By simply placing the bill in the detector, counterfeit currency is immediately identified, without the need for an employee to closely examine the bill.

MATLAB technique: We can split the red, blue, green components of a picture and name them as r1, g1, b1 which correspond to image i.e. original currency note. Consider second image that is note to be tested. Split this image to components r2, b2, g2. Construct a new image with components as r1, g2, b1 or r2, g1, b1 or b2,g1,b1.But r1,g2,b1 combination is most preferred because human eye is sensitive to green component and most of our images contains maximum green component so that our output image will be much easier to identify the fake note more efficiently. Now compare newly constructed image with image1.Calculate the threshold value of equivalence by calculating the standard deviation. If equivalence is above 40% then we can consider it as original note. We consider 40% value because note may be damaged. In addition to these we also apply above specified 10 methods. Parameters for measure of comparing images are Mean Square Error (MSE), Peak Signal to Noise Ratio (PSNR in dB), and structural Content (SC).

VI.CONCLUSION

Using this project, we would detect the fake currency using image processing.This would eliminate the circulation of fake note in the system to some extent.It would provide an opportunity for the user to properly detect the authenticity of note actually without going to the banks.This project discussed a technique for verifying Indian paper currency. This project is an effort to suggest an approach for extracting characteristic of Indian paper currency. Approach suggested from the beginning of image acquisition to converting it to gray scale image and up to the word segmentation has been stated. The work will surely be very useful for minimizing the counterfeit currency. In Future, Mobile app can be developed which would be useful for normal as well as visually impaired persons, the same system can be developed for the remaining Indian currency notes and other country's currency notes. Also the app's interface can be further modified as per the user requirements.In this paper, an efficient approach is proposed to extract the features of Indian currency notes and recognize it. The paper also contains the fake currency detection and authentication. Our future work will be concentrated on extraction of features from various currency notes belonging to different countries as well as recognition and classification. Our future scope will be conversion of currency denomination

VII.REFERENCES

1.Rubeena Mirza1,Vinti Nanda2 "Design and implementation of Indian Paper currency authentication system based on Feature extraction by Edge based Segmentation using sobel operator" International journal of engineering Research and development e-ISSN:2278-067X,p-ISSN:2278-800X, www.ijerd.com Volume 3,Issue 2(august 2012) PP. 41-46

2. Rubeena Mirza, Vinti Nanda, "paper currency verification System Based On Characteristics Extraction Using Image Processing", International Journal of engineering and advanced technology (iJEAT) ISSN 2249-8958, Volume-1, Issue-3,February 2012.

3.Kalyan Kumar Debnath, bSultan Uddin Ahmed,aMd. Shahjahan "A Paper currency Recognition System using negatively correlated Neural network Ensemble", JOURNAL OF MULTIMEDIA, VOL. 5, NO.6, DECEMBER 2010@2010

4.ReserveBank of India-Security Features.

5. Megha Thakur, Amrit Kaur, "VARIOUS FAKE CURRENCY DETECTION TECHNIQUES" International Journal For Technological Research In Engineering Volume 1, Issue 11, pp.1309-1313, July-2014

6.Counterfeit Currency Detection Technique Using Image Processing, Polarization Principle and Holographic Technique(IEEE) By Santhanam, K. ; Dept. of Electron.&Instrum. Eng., Sri Sairam Eng. Coll., Chennai, India ; Sekaran, S. ; Vaikundam,S; Kumarasamy,A.M.

7.Sanjana, ManojDiwakar, Anand Sharma, "An Automated recognition of Fake or Destroyed Indian currency notes in Machine vision", IJCSMS, Vol. 12, April 2012.

8. Hanish Agarwal, Padam Kumar, "Indian currency note denomination recognition in color images", IJACEC, Vol. 1, ISSN 2278–5140.

9. Foresti G.L, Regazzoni C,"A hierarchical approach to feature extraction and grouping" IEEE Trans Image Processing, 2000; 9(6):1056-74.

10. Euisun Choi, Jongseok Lee and JoonhyunYoon,"Feature Extraction for Bank Note Classification Using Wavelet Transform"2006 @ISBN ISSN: 1051-4651, 0-7695-2521-0, IEEE.

11. Peng Wang and Peng Liu, "Invariant Features Extraction for Banknote Classification "Proceedings of the 11th Joint Conference on Information Sciences@2008.

12 Ahmadi and S.Omatu," A Methodology to Evaluate and Improve Reliability in Paper Currency Neuro-Classifiers" Proceedings 2003 IEEE International Symposium on